ADVANCED INSAR COREGISTRATION USING POINT CLUSTERS

Petar S. Marinkovic and Ramon F. Hanssen

DEOS - Delft Institute of Earth Observation and Space Systems, Delft University of Technology, Kluyverweg 1, 2629HS, Delft, The Netherlands, Email: p.s.marinkovic@lr.tudelft.nl

ABSTRACT

Traditional coregistration methods based on correlation optimization, can, due to temporal decorrelation, fail to produce satisfactory results. We propose an alternative method for fine coregistration, which determines the offset vectors by using a cluster of points. The point clusters are realized by means of the modified Harris point detector, and allow a certain refinement in the correlation matching. The first results on real images show that the method alleviates the problem of coregistration of the low coherence scenes with an additional computational overhead.

1. INTRODUCTION

Coregistration is an essential step in the generation of SAR interferograms. Although correlation-based coregistration algorithms have been efficiently implemented in conventional InSAR, in Persistent Scatterer (PS) interferometry, [1], such methods may fail to produce satisfactory results. This is due to the long time separation between acquisitions, which results in a severe temporal decorrelation, [2], and to the, sometimes very large, spatial baselines, resulting in geometric decorrelation, [2]. Conventional correlation-based methods may fail in such "extreme" situations.

The coregistration aims to find an optimal transformational model between master and slave image [3]. Conventional techniques are usually based on the cross-correlation of the squared image amplitudes. The offset vectors, necessary to align the slave image to the master, are computed with sub-pixel accuracy for a number of locations in the master. Over the total image space, for a large number of windows (e.g. 500 windows of size 32×32 pixels or more), the offset between master and slave is estimated by computing the correlation of the magnitude images for shifts at the sub-pixel level. Using these offsets, the two-dimensional coregistration polynomial is computed up to a certain degree.

In order to guarantee an appropriate accuracy under extreme conditions, i.e., master and slave combinations with the large temporal and/or perpendicular baseline, the conventional methods are usually modified by enlarging the size of the correlation window, repositioning the estimation windows, or lowering of the correlation threshold. These modifications are usually performed manually and on a case-to-case basis.

This paper proposes an alternative algorithm for fine InSAR coregistration, which determines the offset vectors by using a cluster of points. Since it does not require a DEM, as proposed by [4], it can be regarded as a modification of the conventional method in terms of a better distribution of the correlation windows. Moreover, the better window distribution allows certain improvements in the correlation matching procedure.

Definition of a cluster of points is performed with a modified Harris point detector, [5], which successfully identifies characteristic points of input image features, i.e., control points. As shown in [6], the intensity-based algorithms for (control) point selection can be successfully implemented in the InSAR processing, guaranteeing a more homogeneous distribution of the correlation windows. Since this distribution directly influences the quality of the coregistration model, it can be better controlled and fine-tuned.

It is well known that nonlinear filters for edge or point detection in image processing are designed for images with additive noise,

$$\underline{y}(x) = s(x) + \underline{e}(x), \tag{1}$$

where $s(x)$ is the (uncorrupted) image signal at position x, $\underline{y}(x)$ is the stochastic observed signal, and $\underline{e}(x)$ is the noise component. Since coherent illumination sources, such as a synthetic aperture radar,

Proc. of the 2004 Envisat & ERS Symposium, Salzburg, Austria 6-10 September 2004 (ESA SP-572, April 2005)

have predominantly multiplicative noise contributions (speckle noise),

$$\underline{y}(x) = s(x) \cdot \underline{e}(x), \tag{2}$$

where the noise is assumed to be stationary with expectation $E\{\underline{e}(x)\} = 1$ and dispersion $D\{\underline{e}(x)\} = \sigma^2$, most conventional filters are usually not as effective as for additive noise. Nevertheless, we perform an empirical analysis to assess the feasibility of the Harris point detector algorithm for radar data, especially for low coherence scenes. Note that the proposed procedure is not intended to replace the conventional correlation approach, but can be used as a backup coregistration tool to be used if the conventional method fails.

In Section 2 we define the intensity-based point detector method as a measure for point selection within SAR scene. In Section 3, a detailed analysis of the modified Harris detector is presented from the perspective of InSAR processing. This analysis is incorporated into a coregistration algorithm to demonstrate the improved results, presented in Section 4 and is followed by a discussion and conclusions in Section 5.

2. INTENSITY BASED METHODS

In the analysis corners and edges are defined as follows.

- *Corners (control points)* of local features (shapes) in a SAR image are characterized by locations where variations of intensity $I(x, y)$ as a function of pixel position are high in both range (x) and azimuth (y) directions. In this case both partial derivatives of I are large, see Fig. 1.
- *Edges* are locations in the SAR image where the variation in intensity $I(x, y)$, as a function of pixel position, in a certain direction is high, while in the corresponding orthogonal direction is low. For an edge oriented along the range axis, this partial derivative is large, while in the azimuth direction it will be low, see Fig. 1.

Here we refer to upper defined corners as the control points.

2.1. Intensity-Based Detector

The main idea behind the intensity-based point detectors is the utilization of the auto-correlation function of the signal, see [7]. In other words, the intensity-based detector measures the intensity differences between a window and windows shifted in several directions, i.e., four discrete shifts in directions parallel to the rows and columns of the image are used. When the minimum of these four differences is greater than the threshold, a control point is detected.

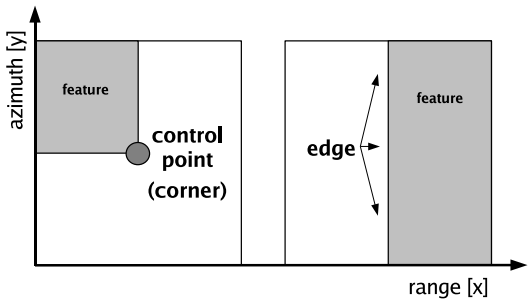

Figure 1. Definitions: Control point (corner) and edge.

Intensity methods are based on a matrix related to the auto-correlation function. This matrix $\mathbf{N}$ averages derivatives of the signal in the window w around a point (x, y).

$$\mathbf{N}(x,y) = \begin{bmatrix} \sum_w (I_x(x_k, y_k))^2 & \sum_w I_x(x_k, y_k) I_y(x_k, y_k) \\ \sum_w I_x(x_k, y_k) I_y(x_k, y_k) & \sum_w (I_y(x_k, y_k))^2 \end{bmatrix}, \tag{3}$$

where $I(x, y)$ is the image function and (x_k, y_k) are the points in the window around (x, y). This matrix captures the structure of the neighborhood. If it is of rank two—that is, both of its eigenvalues are large—a control point is detected. A matrix of rank one indicates an edge and a matrix of rank zero a homogeneous region. The relation between this matrix and the auto-correlation function is given in Appendix A.

2.2. The Harris detector

Harris [5] improved the intensity approach of [7] by using directly the eigenvalues of the auto- correlation matrix $\mathbf{N}$. The use of discrete directions and shifts is thus avoided. Instead of using a simple sum, a Gaussian can optionally be used to weight the derivatives inside the search window. In this way the control points are detected if the auto-correlation matrix $\mathbf{N}$ has two significant eigenvalues. It is important to note that the repeatability and localization of control points are two conflicting criteria, i.e., smoothing improves repeatability but degrades localization [8].

The repeatability rate is a percentage of the total observed points that are detected in both images.

3. ANALYSIS: THE HARRIS POINT DETECTOR

In the following two subsections the application of the Harris detector to InSAR is analyzed, first mathematically and the followed by experiments on real SAR images.

3.1. Theoretical Analysis

As previously indicated, the Harris point detector selects a point for which autocorrelation function significantly drops in two perpendicular directions. That way the control points can be optimally retrieved from SAR scenes. For the decision on the selection of appropriate algorithm for control points detection in SAR images we followed [9].

The intensity-based algorithms presented in [9] were compared in regard to their performance by means of the repeatability rate of the control points selected in the master/slave combination. The tested algorithms were (a) Harris corner detector, (b) Cottier algorithm and (c) Horaud algorithm.

The analysis showed, that even though all the tested algorithms have the same background idea, i.e., the partial derivatives of the intensity, the Harris algorithm produced the best results. Even in the case of master/slave combinations, where a low coherence interferogram is expected, the Harris model came also with good results. Of course, a set of arbitrary parameters has to be adapted for a successful InSAR application, which is later on dealt with in this paper. Due to arbitrariness of the Harris model, which is represented through this set of parameters, the revised Harris model is finally introduced and applied, which has the same properties like the original one. Therefore, the properties of the original Harris measure are reviewed in detail.

The mathematical description of the detector is derived firstly, by computing locally averaged moment matrix from the image gradients and then, by combining the eigenvalues of the (sub-pixel) moment matrix in computation of a corner "strength" whose maximum values indicate the control points. The detection of the control points is based on the derived local structure tensor $\mathbf{N}$, see Appendix A, which represents the local statistics of the first order derivatives around a pixel (x, y):

$$\mathbf{H} = G(\sigma) \otimes \mathbf{N}(x, y) = G(\sigma) \otimes \begin{pmatrix} I_x^2 & I_x I_y \\ I_y I_x & I_y^2 \end{pmatrix} \quad (4)$$

where $G(\sigma)$ is an optional Gaussian with standard deviation σ and $\otimes$ is the convolution operator. The first derivatives I_x and I_y are estimated by convolving the intensity value of the image $I(x, y)$ with the optional smoothing operator in order to reduce noise and aliasing effects. Note that smoothing with the Gaussian, or any other filtering, is not performed on the input images, but on the images containing the squared image derivatives.

The control points are pixels for which $\mathbf{H}$ has two large eigenvalues. The so-called corner response function ("cornerness") R allows a direct control point sub-pixel detection:

$$\begin{aligned} R &= \det(\mathbf{H}) - \alpha \ \mathrm{trace}^2(\mathbf{H}), \quad 0.04 \leq \alpha \leq 0.06 \\ \det(\mathbf{H}) &= \lambda_1 \lambda_2 \\ \mathrm{trace}(\mathbf{H}) &= \lambda_1 + \lambda_2 \end{aligned} \quad (5)$$

The pixel positions of the control points are found at local maxima of R above the given threshold T ($T > 0$). Note that in this case the threshold is on the corner response and not on the intensity value, though the relation between these two components can be derived. The sub-pixel position may be gained by fitting a quadratic approximation to R,

$$a + bx + cy + \frac{1}{2}dx^2 + exy + \frac{1}{2}fy^2 = R(x, y). \quad (6)$$

Using the nine pixels around (x, y) this leads to 9 equations with 6 unknowns which can be trivially solved by a least-squares algorithm, see for example [10].

3.1.1. Eigenvalue Analysis

This subsection summarizes the basic properties of the Harris detector which are realized from the eigenvalue analysis of the local structure matrix, see Eq. (4). As previously indicated, the eigenvalues are incorporated in Eq. (5), which serves as a measure for the control point response.

From Fig. 2, which visualizes the "cornerness" equation, Eq. (5), the following conclusions on the properties of the Harris corner detector algorithm can be drawn.

- *Rotation invariance*: The ellipse rotates but its shape (i.e. eigenvalues) remains the same. Hence, the "cornerness" function R is invariant to rotation.
- *Partial invariance to (affine) intensity change*:
  - Invariance to intensity shift $I \rightarrow I + b$, since only partial derivatives are used in the definition of the local structure matrix;

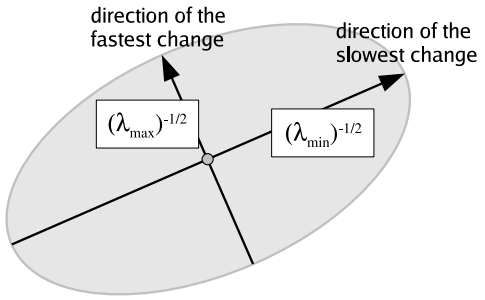

Figure 2. Intensity change in the control point selection window: eigenvalue analysis

– Invariance to intensity scale $I \rightarrow a \cdot I$.

- *Non-invariance to image scale.*

The implemented conditions for the control point selection, using the Harris corner detector algorithm, are listed from the properties of the local structure matrix and "cornerness" function and depicted by Fig. 3.

- R depends only on eigenvalues of $\mathbf{H}$,
- R is large for a control point,
- R is negative with large magnitude for an edge,
- $|R|$ is small for a flat region.

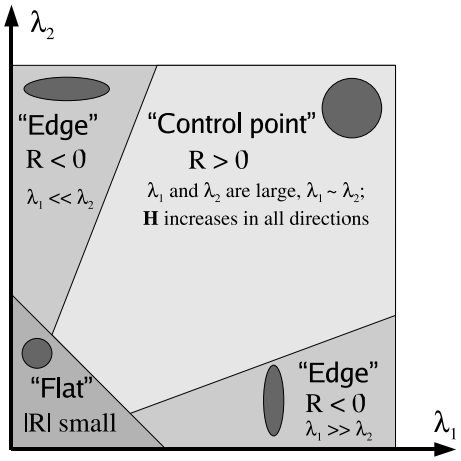

Figure 3. Classification of the control points using eigenvalues of the local structure matrix $\mathbf{H}$ *or the "cornerness" function* R.

3.2. Experimental analysis

This subsection reviews the practical implementation of the Harris detectors on SAR images. Even though the practical application of the Harris detector to InSAR results in a modified detector model, it is important to further elaborate on the parameters of the Harris detector and cornerness function, Eqs. (4) and (5).

The sub-pixel positions of control points are found at local maxima of R above the given threshold T ($T > 0$). For InSAR applications the following arbitrary parameters give the best results, $\alpha = 0.06$ (empirical constant) and for threshold the 25 to 35 times larger value of the maximum intensity inside the cluster window, i.e., input patch. Note that in this case, the threshold is on the corner response and not on the intensity value. The presented values are evaluated on their performance in the control points selection within a test data set of SAR images.

Furthermore, the radar image data are generally highly sensitive to any kind of data smoothing, which makes it important to analyze the application of Gaussian in Eq. (4). The smoothing operator is applied to avoid control points due to image noise, [5]. This is however not done on the input image but on the image window containing the squared intensity derivatives. Therefore, the influence of the Gaussian operator with $\sigma = 1.0$ is experimentally evaluated. The analysis showed that the influence lies within the range of 0.05 to 0.1 pixels. That is, on the limit for the coregistration accuracy of one-eight of the pixel, [11]. Hence, it is recommended to avoid the Gaussian smoothing. For coarse coregistration the influence of smoothing can be disregarded.

3.2.1. The modified Harris point detector

Since the parameters α and σ are arbitrary, they can be always fine tuned for the specific demands on the control points. In order to avoid the arbitrariness of the detector function, Eq. (5), which is represented by the optional parameters, a different model for the Harris corner measure is implemented in the "production" version of the coregistration algorithm:

$$R = \frac{I_x^2 \cdot I_y^2 - (I_x I_y)^2}{I_x^2 + I_y^2 + eps} \tag{7}$$

where *eps* is floating-point relative accuracy. As shown by [12] the modified model possesses the same properties as the original Harris measure. In this implementation the strict definition of the α parameter is avoided, and the lower threshold on the point response can be omitted. A more detailed explanation of the implementation is given in Section 4.

3.2.2. Cluster and point detector window

Another important set of parameters which directly influences the distribution and the number of control points is the size of the cluster and point detector window. The cluster window is the size of the input image patch, while the control point search window is a radius of the region considered in non-maximal suppression, i.e., the distance between two neighboring control points. Even though this set is not parameterized within the cornerness equation, see Eq. (7), the analysis showed that the size of the cluster and control point search window has to be considered and that there is a certain relationship between these two parameters.

It is realized that for urban areas a large patch of 1024×1024 for a cluster window is acceptable, while for non-urban areas the input patch should be smaller by factor 2 or 4. Furthermore, this influences the size of the control point search window. If the cluster window covers a non-urban area, the size of the control point search window should not be more then 5 pixels, in order to detect control points of small features. In an urban area, the control point search window of 10 pixels (or even more) is expected to give good results. The following figures illustrate the influence of the control point window size on their selection and distribution.

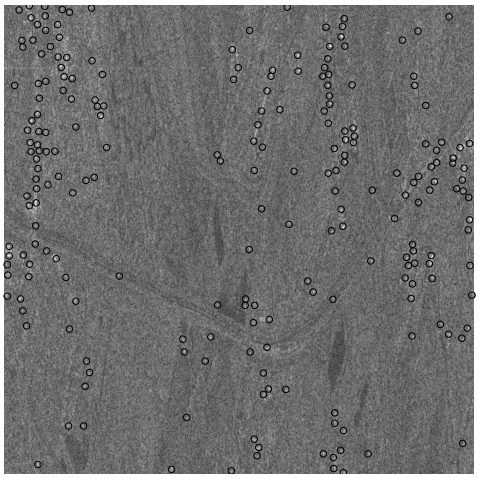

Figure 4. Performance of the control points selection window of the size of 5 pixels.

The comparison between the distribution of points selected by simple thresholding the amplitude and the modified Harris point detector is the final step in the discussion of the implementation of the point detection algorithm. The results, depicted by Figs. 6 and 7, confirm the significantly better performance of the modified Harris algorithm in terms of the spatial distribution of the control points. With this a more homogeneous distribution of the correlation windows is guaranteed, which results in a better quality of the coregistration polynomial, [3].

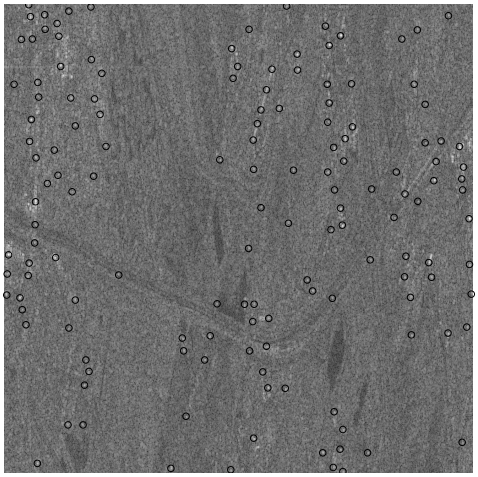

Figure 5. Performance of the control points selection window of the size of 10 pixels.

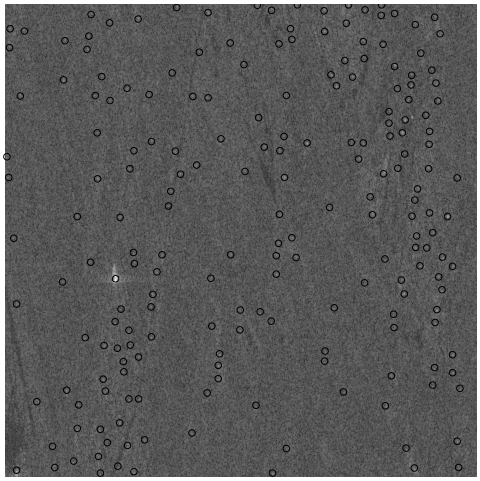

Figure 6. Spatial distribution of points selected with the modified Harris point detector.

4. ALGORITHM IMPLEMENTATION

This section reviews the basic steps in the implementation of the modified Harris detector model within the (fine) coregistration algorithm. As previously indicated, the basic idea of the implementation is the application of image features in the distribution of the correlation windows over the scenes. The distribution is realized through the control points, the characteristic points of the image features, which are detected in both master and slave images. Consequently, these feature points are used for the correlation matching between master and slave. In other words, the control points in both master and slave are used to position the correlation windows. This yields to the modification of the conventional correlation matching step. The final result of the algorithm is the offset vectors map which is used for the computation of the coregistration polynomial.

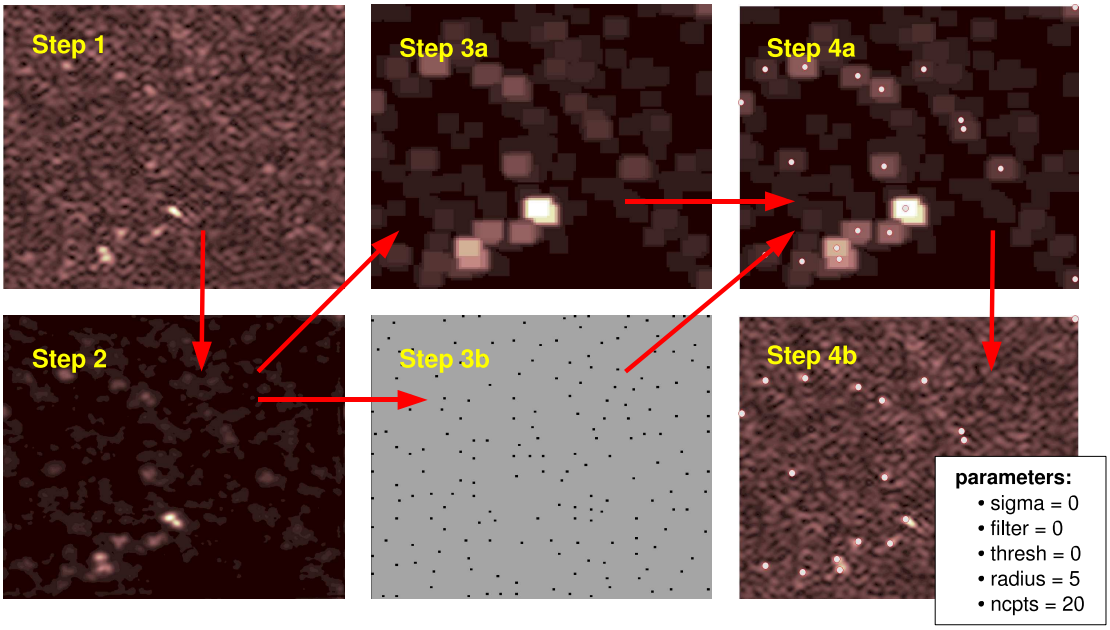

Figure 8. Flowchart of the control points selection algorithm.

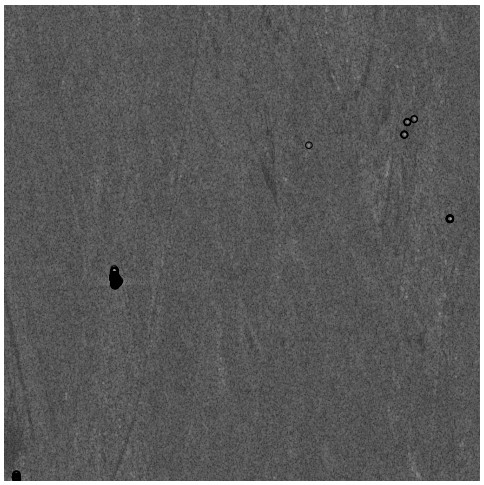

Figure 7. Spatial distribution of points selected by threshold on the amplitude.

4.1. Point Selection

The point selection algorithm flowchart is given in Fig. 8, where each step is visualized with the output (matrix) of that particular step. The following bullet-list gives more information about the each step. Note that for the sake of simplicity and clarity of the images in Fig. 8 the input image is of 128×128 pixels.

- **Step 1 (input):** An input image, usually oversampled by the factor of 2 to avoid aliasing effect, and to improve the localization of the feature point selection.
- **Step 2 (mapping):** Compute the Harris cornerness measure, Eq. (7), which transforms the input image into the control point strength image.
- **Step 3a (radius):** Extract local maxima of the input image by performing a gray scale morphological dilation, see for example [14]. In other words, this matrix is used for points selection within a certain radius from each other.
- **Step 3b (binary):** Binary matrix of control points within the input patch. Optionally, by applying Eq. (6) the sub-pixel position of the control points can be determined. The control point search window is a radius of the region considered in non-maximal suppression, i.e., the distance between two neighboring control points.
- **Steps 4a and 4b (output):** Control points are located by finding points in the control point strength image that match the dilated image and are also greater than a certain threshold. The input value for the threshold can be omitted by setting the number of control points requested from the input patch, e.g., the number of points is 20.

4.2. Correlation Matching

In this step of the coregistration algorithm the offset vector map between the input images is generated. The offset map is computed from previously detected control points in two input images, by looking for points that are maximally correlated with

each other within windows surrounding each point. The points that correlate most strongly with each other in "both" directions are returned as an output. This is a simple N^2 comparison.

Furthermore, only the control points within a certain disparity limit are compared over the two input images. The disparity limit (max/min) can be set by using an output of the coarse coregistration step. In the absence of *a priori* information this maximum search radius can be set to max-disparity pixels, i.e., the size of the patch.

In the course of the matching process there are often several candidate matches for each control point. Initially, the one that is the most correlated in image intensities at the control point locations is selected. A normalized cross-correlation of image intensity is used as the measure of the strength of the match. The correlation is performed over two $w \times w$ pixel patches centered on each control point, [13]. In this implementation it is assumed that both input images have a zero mean. Optionally, an image smoothed with an averaging filter (see for example [14]) of size $w \times w$ is subtracted from each of the input images, Fig. 9. This filtering compensates for brightness differences in each image and allows faster correlation calculation.

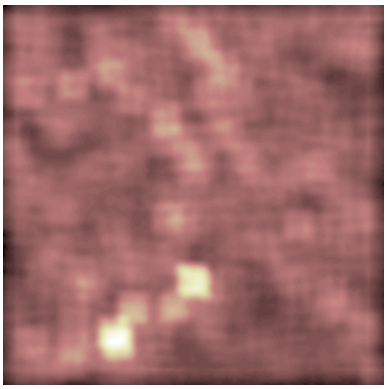

Figure 9. Visualization of the average filter of size $w = 5$ for the input image of Fig. 8.

The maximum strength matches are stored for each control point from the first to second image in the form of a correlation matrix, Fig. 10. The correlation matrix holds the correlation strength of every point relative to every other point. This is necessary to find pairs of points that correlate maximally in both directions. Matches are accepted into the initial set of offset vectors, if they exhibit a maximum in both directions. This has the effect of removing control points which are ambiguous in that they have multiple candidate matching.

For the analysis of the correlation matrix, a maximum is found along rows (azimuth direction) that gives the strongest match in the array of control points of the slave image for each member of the

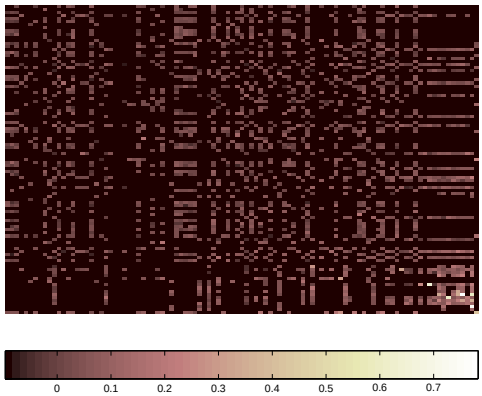

Figure 10. Correlation matrix: For every feature point in the first image a window of data is extracted and correlated with a window corresponding to every feature point in the other image.

array of control points of master image. Secondly, the same procedure is performed along the columns (range direction). The maximum value down the columns give the strongest match in points array of master for each point of the slave set. Finally, matches which were consistent in both directions are found and extracted from original arrays to form the initial offset vector map, see Fig. 11

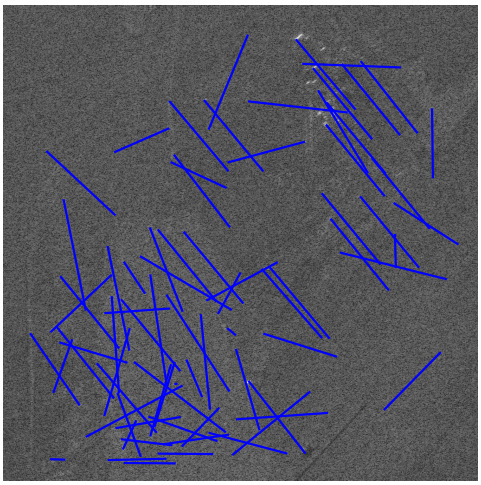

Figure 11. Initial set of offset vectors.

Finally, the initial set of offset vectors is tested for outliers (e.g., data-snooping, [10]) to result with the final offset map, Fig. 12, which is subsequently used for the computation of the coregistration polynomial.

5. CONCLUSIONS

A methodology using unconventionally detected point clusters for SAR image coregistration is developed, by using the modified Harris point detector. This method is intended to be used as an alternative

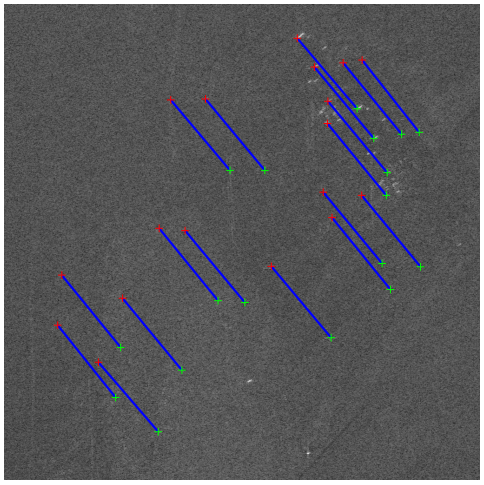

Figure 12. Final set of offset vectors.

for conventional, correlation-based, coregistration algorithms in cases where correlation between the two image scenes is extremely low, e.g., due to temporal decorrelation or baselines longer than the critical baseline.

The main advantages of this method are: (a) a successful application of the image features, (b) a direct comparison between master and slave image, and (c) coarse coregistration can be omitted. A potential drawback of this approach could be a demanding computation time. Also, more parameters are required for fine-tuning as well as a special care with optional data filtering and smoothing is required.

The evaluation of the quality and performance of the method is limited to a few case studies. In fact, it is difficult to assess the performance, because on one hand, both methods perform well in a "normal" situation case, but on the other hand, in "extreme" cases, where the conventional method usually fails to give reasonable results, there is no ground for a comparison.

Nevertheless, it is anticipated that the method performs in an "extreme" situation case at least as accurate as the conventional. The reasoning behind this is, that the refinement provided with the presented coregistration model enables:

1. the correlation windows to be more "accurate", by the homogeneous point distribution and the direct comparison between master and slave image;
2. the points which would result with a low correlation are used more efficiently in the offset estimation, by using the sub-pixel correlation matrix

It is also important to stress that this model is designed as an alternative and not as a replacement tool for conventional coregistration methods.

APPENDIX A: DERIVATION OF THE AUTO-CORRELATION MATRIX

The local auto-correlation function measures the local changes of the signal. This measure is obtained by correlating a patch with its neighboring patches, that is with patches shifted by a small amount in different directions. In the case of a control point, the auto-correlation function is high for all shift directions.

Given a shift $(\Delta x, \Delta y)$ and a point (x, y), the auto-correlation function is defined as:

$$f(x,y) = \sum_w (I(x_k, y_k) - I(x_k + \Delta x, y_k + \Delta y))^2, \quad (8)$$

where (x_k, y_k) are the points in the window w centered on (x, y) and I the image function.

To detect control points we have to integrate over all shift directions. Integration over discrete shift directions can be avoided by using the auto-correlation matrix. This matrix is derived using a first-order approximation based on the Taylor expansion:

$$\begin{aligned} & I(x_k + \Delta x, y_k + \Delta y) \\ & \approx I(x_k, y_k) + (I_x(x_k, y_k) I_y(x_k, y_k)) \begin{pmatrix} \Delta x \\ \Delta y \end{pmatrix} \end{aligned} \quad (9)$$

Substituting the above approximation into Eq. (8), we obtain:

$$\begin{aligned} f(x,y) &= \sum_w \left((I_x(x_k, y_k) \quad I_y(x_k, y_k)) \begin{pmatrix} \Delta x \\ \Delta y \end{pmatrix} \right)^2 \\ &= (\Delta x \quad \Delta y) \cdot \\ &\quad \begin{bmatrix} \sum_w (I_x(x_k, y_k))^2 & \sum_w I_x(x_k, y_k) I_y(x_k, y_k) \\ \sum_w I_x(x_k, y_k) I_y(x_k, y_k) & \sum_w (I_y(x_k, y_k))^2 \end{bmatrix} \cdot \\ &\quad \begin{pmatrix} \Delta x \\ \Delta y \end{pmatrix} \\ &= (\Delta y \quad \Delta x)\, \mathbf{N}(x,y) \begin{pmatrix} \Delta x \\ \Delta y \end{pmatrix}, \end{aligned} \quad (10)$$

which shows that the auto-correlation function can be approximated by the matrix $\mathbf{N}(x, y)$, which captures the structure of the local neighborhood.

REFERENCES

[1] A. Ferretti, C. Prati, and F. Rocca. Permanent scatterers in SAR interferometry. *IEEE Transactions on Geoscience and Remote Sensing*, vol. 38, 5:2202–2212, September 2000.

[2] H.A. Zebker and J. Villasenor. *Decorrelation in interferometric radar echoes. IEEE Transactions on Geoscience and Remote Sensing*, vol. 30, 5:950–959, September 1992.

[3] R. Hanssen. *Radar Interferometry: Data Interpretation and Error Analysis.* Kluwer Academic Publishers, 2001.

[4] N. Adam, B.M. Kampes, M. Eineder, et. al. The development of a scientific permanent scatterer system. In *Proceedings of ISPRS Workshop High Resolution Mapping from Space, Hannover, Germany, 2003*, 6 pages, 2003.

[5] C.J. Harris and M. Stephens. A combined corner and edge detector. *Proc. 4th Alvey Vision Conf.*, pages 147–151, 1988.

[6] P.S. Marinkovic and R.F. Hanssen. Advanced InSAR coregistration using point clusters. In *International Geoscience and Remote Sensing Symposium, Anchorage, Alaska, 20-24 September 2004*, pages 4, cdrom, 2004

[7] H.P. Moravec. Towards automatic visual obstacle avoidance. In *Proceedings of the 5th International Joint Conference on Artificial Intelligence, Cambridge, Massachusetts, USA*, page 584, 1977.

[8] J. Canny. A computational approach to edge detection. *IEEE Transactions on Pattern Analysis and Machine Intelligence*, vol. 8, 6:679–698, 1986

[9] C.S. Schmid, R. Mohr, and C. Bauckhage. Evaluation of Interest Point Detectors. *International Journal of Computer Vision*, vol. 37, 2:157–172, June 2000.

[10] P.J.G. Teunissen. *Adjustment theory; an introduction, 1st ed.* Delft University Press, Delft, 2000.

[11] R. Bamler and D. Just. Phase statistics and decorrelation in SAR interferograms. In *Proceedings IGARSS 1993*, pages 980–984, 1993.

[12] J. Noble. Finding corners. *Image and Vision Computing Journal*, vol. 6, 2:121–128, May 1988.

[13] L.G. Brown. A Survey of Image Registration Techniques. *ACM Computing Surveys*, vol. 24, 4:325–376, December 1992.

[14] J.S. Lim. *Two-Dimensional Signal and Image processing.* Prentice-Hall International, London, 1983.

[15] B. Kampes, R. Hanssen, and Z. Perski. Public domain tools in radar interferometry. In *Third International Workshop on ERS SAR Interferometry, 'FRINGE03', Frascati, Italy, 3-5 Dec 2003*, page cdrom, 9 pages, 2003